JMEPEG (2003) 12:597-601 ©ASM International

Effect of Austenitization on Austempering of Copper Alloyed Ductile Iron

Uma Batra, S. Ray, and S.R. Prabhakar

(Submitted 8 February 2003)

A ductile iron containing 0.6% copper as the main alloying element was austempered at a fixed austempering temperature of 330 °C for a fixed austempering time of 60 min after austenitization at 850 °C for different austenitization periods of 60, 90, and 120 min. The austempering process was repeated after changing austenitization temperature to 900 °C. The effect of austenitization temperature and time was studied on the carbon content and its distribution in the austenite after austenitization. The effect of austenitization parameters was also studied on austempered microstructure, structural parameters like volume fraction of austenite, X_γ, carbon content C_γ, and $X_\gamma C_\gamma$, and bainitic ferrite needle size, d_α after austempering. The average carbon content of austenite increases linearly with austenitization time and reaches a saturation level. Higher austenitization temperature results in higher carbon content of austenite. As regards the austempered structure, the lowering austenitization temperature causes significant refinement and more uniform distribution of austempered structure, and a decrease in the volume fraction of retained austenite.

Keywords alloyed ductile iron (ADI), austenization, copper

1. Introduction

The steadily increasing interest in the study and development of austempered ductile iron (ADI) is due to its outstanding mechanical properties[1-4] resulting from unique microstructure.[5,6] Commonly ADI is produced by austenitization of ductile iron in the temperature range of 850-950 °C for about 1-1.5 h followed by austempering at temperatures 250-425 °C and then water quenching or air cooling. During austenitization, the cast microstructure transforms to austenite and its carbon content depends upon the initial microstructure including nodule size and nodule count, austenitization temperature, and time. In a fully ferritic matrix, carbon diffuses only from the graphite nodules to the surrounding matrix during austenitization. However, in a pearlitic matrix, the graphite nodule and the cementite of pearlite contribute to the carbon enrichment of the mother austenite,[7] which is subsequently subjected to austempering at a given temperature, taking place in two stages. In stage I, the matrix austenite, γ_o, with carbon content C_γ^o transforms isothermally to acicular ferrite and stabilized austenite, γ, enriched with a carbon content, C_γ. In stage II, which begins at time $t_2>t_1$, the stabilized austenite, γ, decomposes to ferrite and carbide.

The desired austempered microstructure is obtained in the time interval between t_1 and t_2 as it exhibits an optimum combination of mechanical properties.[8]

For commercial exploitation of ADI, it is necessary to establish the heat treatment parameters (i.e., austenitization and austempering temperatures) and times to achieve a wide time period t_2-t_1, called processing window, to obtain an optimum combination of mechanical properties. The effect of austenitization temperature and time on the microstructure of differently alloyed ADI has been studied for different heat-treatment condition.[9-12] Raising the austenitization temperature results in coarser austenite with higher carbon content and increasing austempering temperature results in coarser microstructure with higher carbon content. Present work aims to develop an ADI alloyed with copper for improvement of austemperability along with manganese in commercially viable range of 0.22-0.23-wt.%. Copper has been chosen, as it does not segregate, leading to non-uniform austempered structure.

The study reported here deals with the effect of austenitization temperature and time on the average carbon content and its distribution in austenite matrix before austempering. The

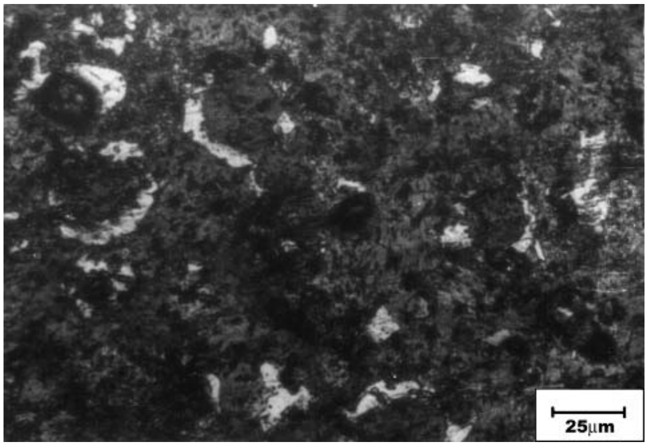

Fig. 1 Microstructure of cast copper alloyed ductile iron

Uma Batra, Dept. of Metallurgical Engineering, Punjab Engineering College Chandigarh, India; **S. Ray,** Dept. of Materials and Metallurgical Engineering, IIT Roorkee, India; and **S.R. Prabhakar,** Rayat Engineering College, Punjab, India. Contact e-mail: umabatra2@yahoo.com.

effects of variation of austenitization temperature and time on austempered microstructure, the amount of retained austenite, X_γ, the average carbon content of retained austenite, C_γ, and the particle size of bainitic ferrite, d_α, have been investigated.

2. Experimental Procedure

A ductile iron of composition (3.48C, 2.028Si, 0.22Mn, 0.05Cr, 0.016Ni, 0.6Cu, 0.04Ti, 0.03Mo, 0.0079Sn, 0.012V, 0.02Al, and rest Fe) was prepared in a commercial foundry using an induction-melting furnace and cast in the shape of 1″ Y block. The cast microstructure is shown in Fig. 1. The microstructural characteristics are given in Table 1. Samples of size 10 × 10 × 15 mm were austenitized at 850 and 900 °C for 15, 30, 60, 90, and 120 min, packed in beds of cast iron chips, and subsequently quenched in water. X-ray diffraction was used to determine the carbon content of austenite.[13] Unnotched-charpy specimens (55 × 10 × 10) mm as per ASTM specifications A 327-80[14] machined from the leg part of Y block castings were austenitized at 850 and 900 °C for three time periods of 60, 90, and 120 followed by austempering in a salt bath held at preselected temperature for different time periods before quenching in water. Samples for metallography were polished, etched, and examined using standard metallographic techniques. The average amount of austenite, X_γ, and its average carbon content, C_γ, and the size of bainitic ferrite particles were found by x-ray diffraction taken with CuKα radiation ($\lambda = 1.54$ A°), and by using the Scherrer formula.[15]

Table 1 Micro Structural Characteristics of Cast Copper Alloyed Ductile Iron

Characteristics	Cu-Iron
Nodule size, mm	0.04
Nodule count	250
Amount of ferrite, %	5
Amount of pearlite, %	95

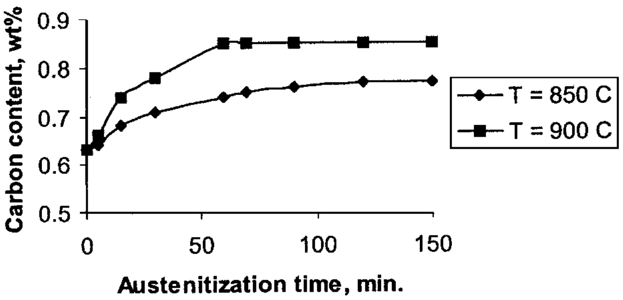

Fig. 2 Variation of carbon content of matrix austenite with austenitization time

3. Results and Discussion

The microstructure of cast Cu-alloyed ductile iron contains graphite nodules in a ferritic-pearlitic matrix (Fig. 1). The effect of austenitization temperature and time on the carbon content and its distribution in austenite has been studied to find appropriate austenitization process variables of temperature and time, which will result in fairly uniform distribution of carbon in austenite.

Austenitization occurs by nucleation and growth. The austenite phase generally nucleates at the ferrite/graphite interface in ductile iron and also at the ferrite-carbide interface if the matrix contains pearlite. The diffusion of carbon to austenite may take place by dissolution of graphite and cementite from nodules and pearlite, respectively. The extent of diffusion depends on austenitization temperature, austenitization time, nodule count, matrix structure, diffusivity of carbon, alloy content, and its segregation in irons. For a given iron at a particular austenitization temperature, T_γ, the austenitization time, t_γ, dictates the carbon content and its distribution in austenite, until equilibrium is reached.

Figure 2 shows the variation of carbon content of austenite with austenitization time, t_γ, for two austenitization tempera-

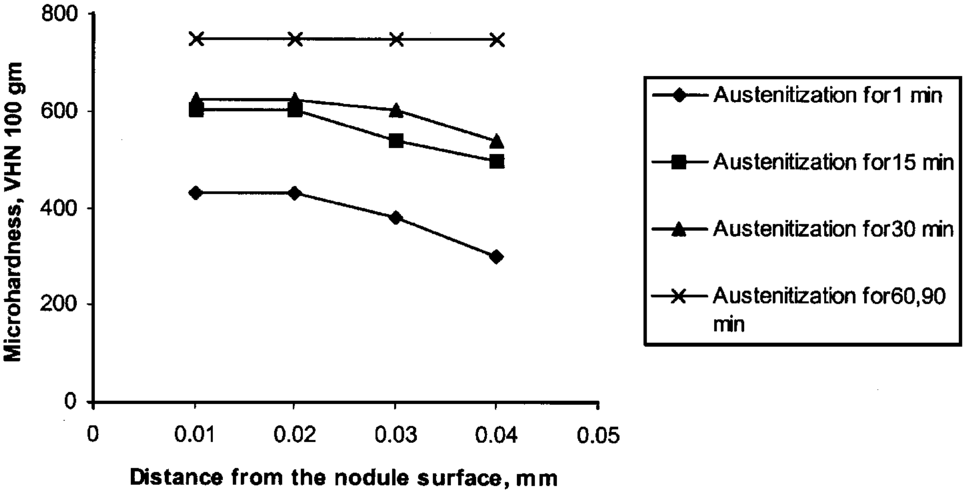

Fig. 3 Variation of Vickers microhardness along the distance from the nodule surface to the middle of the distance between two nodules in austenite matrix of copper alloyed ductile iron after quenching (T_γ = 900 °C, t_γ= 1, 5, 15, 30, 60, 90, and 120 min)

tures of 850 and 900 °C. The average carbon contents of austenite increases linearly with austenitization time and reaches a saturation level of 0.77% after $t_\gamma = 120$ min at $T_\gamma = 850$ °C. The carbon dissolution in austenite is faster at higher austenitization temperatures of 900 °C but the equilibrium saturation level is also higher. The following equation[16] has been frequently used for calculating equilibrium carbon content of austenite:

$$C_\gamma^{o} = (T_\gamma/420) - (0.17 \times \%\ \mathrm{Si}) - 0.95 \qquad \text{(Eq 1)}$$

The present observation of the equilibrium carbon content agrees well with those estimated by Eq 1. The distribution of carbon in austenite has been studied indirectly through micro hardness measurements of matrix between two graphite nodules as observed after austenitization for different times followed by quenching. The minimum time to achieve uniform hardness of the matrix is 120 and 60 min for austenitization temperature of 850 and 900 °C, respectively (Fig. 3). Thus, these time periods are enough for complete austenitization.

Figure 4 shows the variation of austempered microstructure with austenitization at 850 °C for time periods of 60, 90, and 120 min followed by austempering at 330 °C for 60 min. The austempered microstructures consist of bainitic ferrite and retained austenite but it is non-uniform when austempered after 60 or 90 min of austenitization at 850 °C. Non-uniform carbon distribution in the starting austenite before austempering may have contributed to non-uniform austempered structure. As the time of austenitization is increased to 120 min, the bainitic ferrite and retained austenite get distributed more uniformly due to homogeneous carbon content of austenite in the matrix (Fig. 3). However, for the same austempering treatment after austenitization at 900 °C for 60, 90, and 120 min, the microstructures are significantly different from those for austenitization at 850 °C (Fig. 5).

The austempered structure is uniform for 60 min of austenitization, as the carbon content has become uniform after 60 min due to higher diffusion coefficient at 900 °C. The level of carbon is also relatively higher at 0.85 wt.% compared with 0.77 wt.% observed at the lower austenitization temperature of 850 °C. The austempered microstructure is marginally coarser with bainitic ferrite size of 190 A^{o} compared with 185 A^{o} observed for austenitization at 850 °C for 120 min. As the time of austenitization is increased, the resulting austempered microstructure becomes coarser, which may be attributed to grain growth of austenite resulting in lower rate of heterogeneous nucleation of ferrite. Thus, a coarse structure results with retained austenite present as large blocky areas with some martensite in it. The changes in austenite volume fraction, X_γ, and its average carbon content, C_γ, increase with increasing austenitization time, but the size of bainitic needles, d_α, increases only marginally (Table 2). However, when $T_\gamma = 900$ °C, the X_γ increases marginally with increasing t_γ from 60-120 min but its carbon content, C_γ, is observed to decrease. The size of bainitic ferrite increases from 190-239 A^{o}.

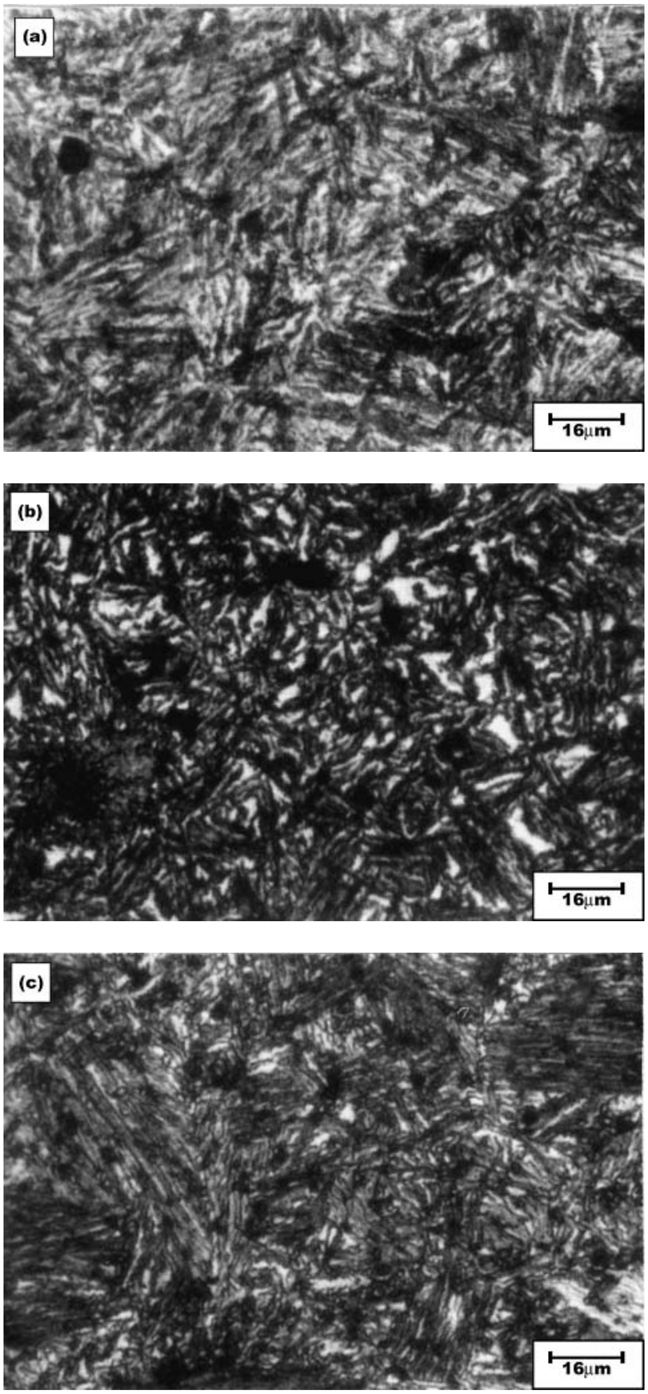

Fig. 4 Microstructure of copper alloyed ADI obtained on austempering for 60 min at a fixed austempering temperature, $T_A = 330$ °C after austenitization at $T_\gamma = 850$ °C for different times, t_γ: **(a)** 60, **(b)** 90, and **(c)** 120 min

The effect of austenitization temperature on the microstructure has been studied by comparing the micrographs in Fig. 4 and 5 for similar austenitization times of 60, 90, or 120 min. The increase in the austenitization temperature from 850-900 °C influences the austempered microstructure in various ways. The austempered microstructure has coarsened, the volume fraction of retained austenite has increased, and the amount of blocky retained austenite has increased. The number of ferrite platelets is much greater for the samples austenitized at 850 °C than those at 900 °C for the same austempering conditions of 330 °C for 1 h as observed in Fig. 4 and 5. A

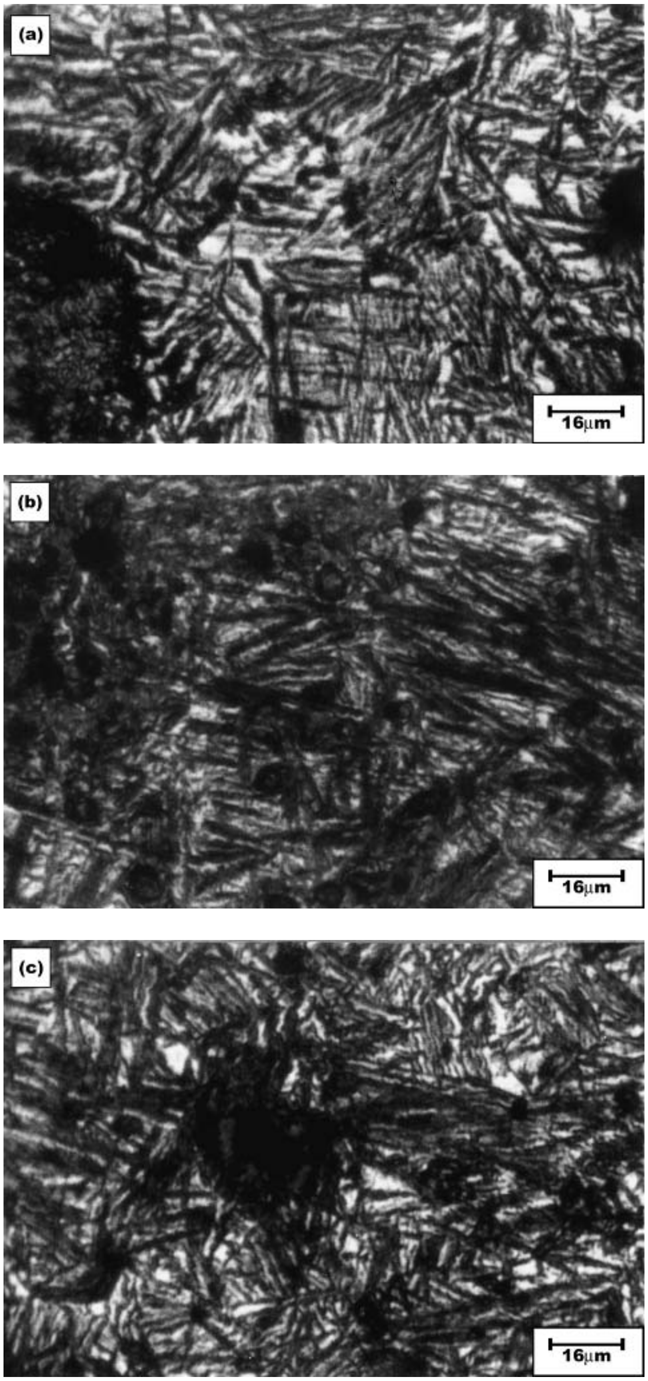

Fig. 5 Microstructure of copper alloyed ADI obtained on austempering for 60 min at a fixed austempering temperature, T_A = 330 °C after austenitization at T_γ = 900 °C for different times, t_γ: **(a)** 60, **(b)** 90, and **(c)** 120 min

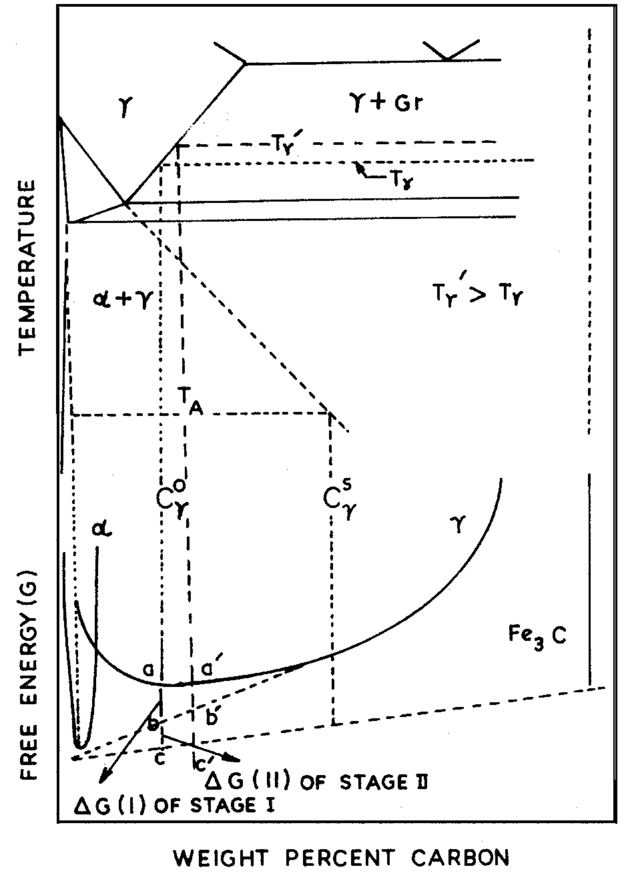

Fig. 6 Schematic free energy-composition diagram indicating the driving force for stage I and stage II of austempering

Table 2 Variation in Austempered Austenite and the Size of Bainitic Ferrite With Austenitization Temperature and Time of Cu Alloyed ADI Austempered at 330 °C and Austempering Time of 60 Min

T_γ, °C	t_γ, Min	Avg, Volume Fraction, X_γ	Avg, C_γ Wt.%	Product, $X_\gamma C_\gamma$	Bainitic Ferrite Particle Size, d_α, A°
850	60	0.25	1.6	0.4	174
850	90	0.31	1.7	0.527	180
850	120	0.33	1.8	0.594	185
900	60	0.36	1.8	0.648	190
900	90	0.37	1.7	0.629	212
900	120	0.38	1.65	0.627	239

logical explanation for the greatly increased number of bainitic ferrite nuclei and more rapid stage I process for the iron austenitized at relatively lower austenitization temperature and carbon content in the starting austenite can be obtained by referring to the schematic free energy-composition diagram in Fig. 6. This figure shows that when austenitization temperature is reduced to T_1, there is corresponding reduction in austenite carbon content. This results in greater driving force (a'-b') for the transformation to metastable product phases α+γ than that for higher austenitization temperature. A greater driving force (a'-b') can affect the rate of stage I in two ways: the number of ferrite nuclei may increase directly and/or the activity gradient driving carbon diffusion may increase. Thus, the transformation to bainitic product occurs more rapidly with decreasing austenitization temperature. At first glance, it appears to be advantageous to increase driving force further by decreasing austenitization temperature. However, care is needed, because as the austenitization temperature decreases, the austenite carbon content (before austempering) decreases and it will result in lower stability of austempered austenite. The magnitude of $C_\gamma X_\gamma$ for austenitization of 900 °C (Table 2), is more than that for the austenitization of 850 °C.

4. Conclusions

The average carbon content of austenite increases with austenitization time and reaches a saturation level. Increasing the austenitization temperature accelerates the austenitization kinetics and increases the carbon content of the resulting austenite. The optimum austenitization time is that at which austenite with maximum and uniform carbon has been achieved. At austenitization temperatures of 850 and 900 °C, the austenitization time corresponding to most desirable austempered microstructure is 120 and 60 min, respectively, for the present ductile iron and the corresponding equilibrium carbon content of austenite is 0.77 and 0.85. Longer austenitization time results in coarse austempered microstructure containing blocky austenite containing some martensite within it. It could be attributed to grain coarsening of austenite in the context of transformation during austempering. Decreasing the austenitization temperature results in relatively finer microstructure with more distribution of phases.

References

1. M. Grech: "An Update on Austempered Ductile Iron" in *International Conference on Mechanical Behaviour of Ductile Cast Iron and Other Cast Metals,* Kitakyushu, Japan, Aug. 1993, pp. 18-25.
2. P.A. Blackmore and R.A. Harding: "The Effects of Metallurgical Process Variables on the Properties of Austempered Ductile Iron" in *Proc. 1st Int. Conf. on ADI*, 1984, pp. 117-34.
3. D.J. Moore, T.N. Rouns, and K.B. Rundman: "The Relationship Between Microstructure and Tensile Properties in ADI," *AFS Trans.*, 1987, pp. 765-74.
4. J. Aranjbal, I. Gutierrez, J.M. Rodriguez-Ibabe, and J.J. Urocla: "Influence of Heat Treatments on Microstructure and Toughness of Austempered Ductile Iron," *Mater. Sci. Technol.*, 1992, (11), pp. 263-73.
5. E. Dorazil, B. Barta, E. Munsterova, L. Stransky, and A. Huvar: "High-Strength Bainitic Ductile Cast Iron," *AFS Int., Cast. Met. J.*, 1982, *2*(7), pp. 52-62.
6. R.B. Gundlach and J.F. Janowak: "Austempered Ductile Iron Combines Strength With Toughness and Ductility," *Met. Prog.*, 1988, pp. 19-26.
7. B. Kovacs: "Austempered Ductile Iron Fact and Fiction," *Modern Cast.*, 1990, pp. 38-41.
8. H. Ali and R. Elliott: *Mater. Sci. Technol.*, 1996, *12,* p. 679.
9. M. Grech and J.M. Young: "Influence of Austempering Temperature on the Characteristics of Austempered Ductile Iron Alloyed with Cu and Ni," *AFS Trans.*, 1990, *98,* p. 345.
10. N. Murakami, R. Kobayashi, and T. Owadano: *Jrn. of JFS*, 1984, *12*(56), pp. 746-51.
11. T.N. Rouns, D.J. Moore, and K.B. Rundman: "On the Structure and Mechanical Properties of Austempered Ductile Iron," *AFS Trans.*, 1984, *92,* pp. 815-40.
12. K. Ogi, A. Sawamoto, Y.C. Jin, and C.R. Loper: "A Study of Some Aspects of the Austenitization Process of Spheroidal Graphite Cast Iron," *AFS Trans.*, 1998, *2,* pp. 75-82.
13. B.D. Cullity: *Elements of X-Ray Diffraction*, Addison Wesley Publishing Company, 1956, pp. 390-96.
14. K.D. Mills: "Spheroidal Graphite Cast Iron—Its Development and Future," *Br. Foundryman*, 1972, *65*, p. 34.
15. K.L. Hayrynen, D.J. Moore, and K.B. Rundman: *Private communication,* 1993.
16. R.C. Voigt and C.R. Loper: "Austempered Ductile Iron—Process Control and Quality Assurance," *J. Heat Treat.*, 1984, *4*(3), p. 291.